Thermal relaxation rates of magnetic nanoparticles in the presence of magnetic fields and spin-transfer effects

William Rippard,[*] Ranko Heindl, Matthew Pufall, Stephen Russek, and Anthony Kos

National Institute of Standards and Technology, Boulder, Colorado 80305, USA

We have measured the relaxation time of a thermally unstable ferromagnetic nanoparticle incorporated into a magnetic tunnel junction (MTJ) as a function of applied magnetic field, voltage V (-0.38 V $< V < +$ 0.26 V), and temperature (283 K $< T <$ 363 K). By analyzing the results within the framework of a modified Néel-Brown formalism, we determine the effective attempt time of the nanoparticle and also the bias dependences of the in-plane and out-of-plane spin-transfer torques. There is a significant linear modification of the effective temperature with voltage due to the in-plane torque and a significant contribution of a "field-like" torque that is quadratic with voltage. The methods presented here do not require complicated models for device heating or calibration procedures but instead directly measure how temperature, field, and voltage influence the energy landscape and thermal fluctuations of a two-state system. These results should have significant implications for designs of future nanometer-scale magnetic random access memory elements and provide a straightforward methodology to determine these parameters in other MTJ device structures.

PACS number(s): 75.75.Jn, 85.75.Dd, 72.25.Ba

I. INTRODUCTION

Accurate and robust methods to determine fundamental parameters associated with nanoscale magnetic structures have been of significant interest within the magnetics community for a number of years. For both magnetic random access memory devices (MRAM) and the hard-disk drive industry, understanding thermal relaxation rates as well as the effects of the spin-transfer torque[1–4] (STT) have become increasingly important as device and bit dimensions shrink. Individual magnetic elements must be thermally stable for data retention, while the writing process is generally strongly influenced by thermal fluctuations even at nanosecond switching times. Spin-transfer effects are expected to enable future scaling of MRAM devices. However, there remains substantial uncertainty[5–17] in the functional dependence of the spin-transfer torque on voltage. Here we demonstrate that we are able to quantitatively determine this dependence and the effective attempt time by measuring the thermal relaxation times (dwell times) of an individual superparamagnetic nanoparticle over a range of temperatures and as functions of applied field and voltage. This method is distinct from other room-temperature (RT) methods previously reported and so provides an independent measurement of these parameters.

Numerous techniques have been used to determine the effective attempt time τ_0 of magnetic nanoparticles, including single domain modeling at finite temperature,[18] measurement of the relaxation rates at $T \approx 4$ K,[19,20] scanning tunneling microscopy studies,[21] and modeling of the RT field[22] or STT switching distributions,[23] among others. The reported values for τ_0 range over many orders of magnitude (10^{-15} s to 10^{-9} s). While theoretical models predict some variation in τ_0 due to its dependence on the magnetic properties of the device under study (e.g., anisotropy, damping, and saturation magnetization)[24] and temperature, it is difficult to reconcile this wide range of values with these predictions. In addition, many of the methods are taken at parameter extremes (low temperature, high voltage), making the extrapolation back to the device operating point uncertain and model dependent.

Here we report on direct measurements of the relaxation times of magnetic nanoparticles at RT and low voltage to determine the effective attempt time of nanoparticles that strongly resemble those relevant to MRAM devices and patterned bits for magnetic recording.

Similarly, many methods have been employed to determine the contributions of the "in-plane" and "field-like" torque terms associated with the STT effect, including modeling the ferromagnetic resonance (FMR) frequency and linewidth changes associated with applied bias,[8–11] extraction from the size and symmetry of a rf current rectified by the magnetic tunnel junction (MTJ) itself,[12–15] determination from the phase relationship between the magnetization direction of a nanoparticle driven by an rf current,[16] and from the voltage-dependent coercivity of an MTJ.[17] The reported results have ranged from the field-like torque being completely linear with V to being completely quadratic in V. In addition, some models have ignored heating effects, while the models that have attempted to include them have been forced to apply macroscopic heat transport theories to nanoscale objects. In the following, we quantitatively determine the in-plane and field-like STT dependencies on voltage from measurements of the relaxation times of magnetic nanoparticles at RT as a function of applied voltage. As we show below these results are, in general, robust with respect to model and heating effects and identify where improvements in the modeling are possibly required.

II. EXPERIMENTAL RESULTS

The device studied here is etched from a MTJ stack consisting of Si substrate/SiO$_2$/TaCu(70)/PtMn(20)/CoFeB(2.5)/ Ru(0.8) / CoFeB(2.5) / MgO(1.0)/CoFeB(2.5)/Ta(10)/Ru(5) (all thicknesses in nanometers) having a tunneling magnetoresistance (TMR) value of $\approx$110% at RT. We pattern the free layer of the device into a nominally 60 × 90 nm^2 ellipse through electron beam lithography and ion milling. The ion milling is stopped within (or just past) the MgO, leaving the pinned synthetic-antiferromagnetic
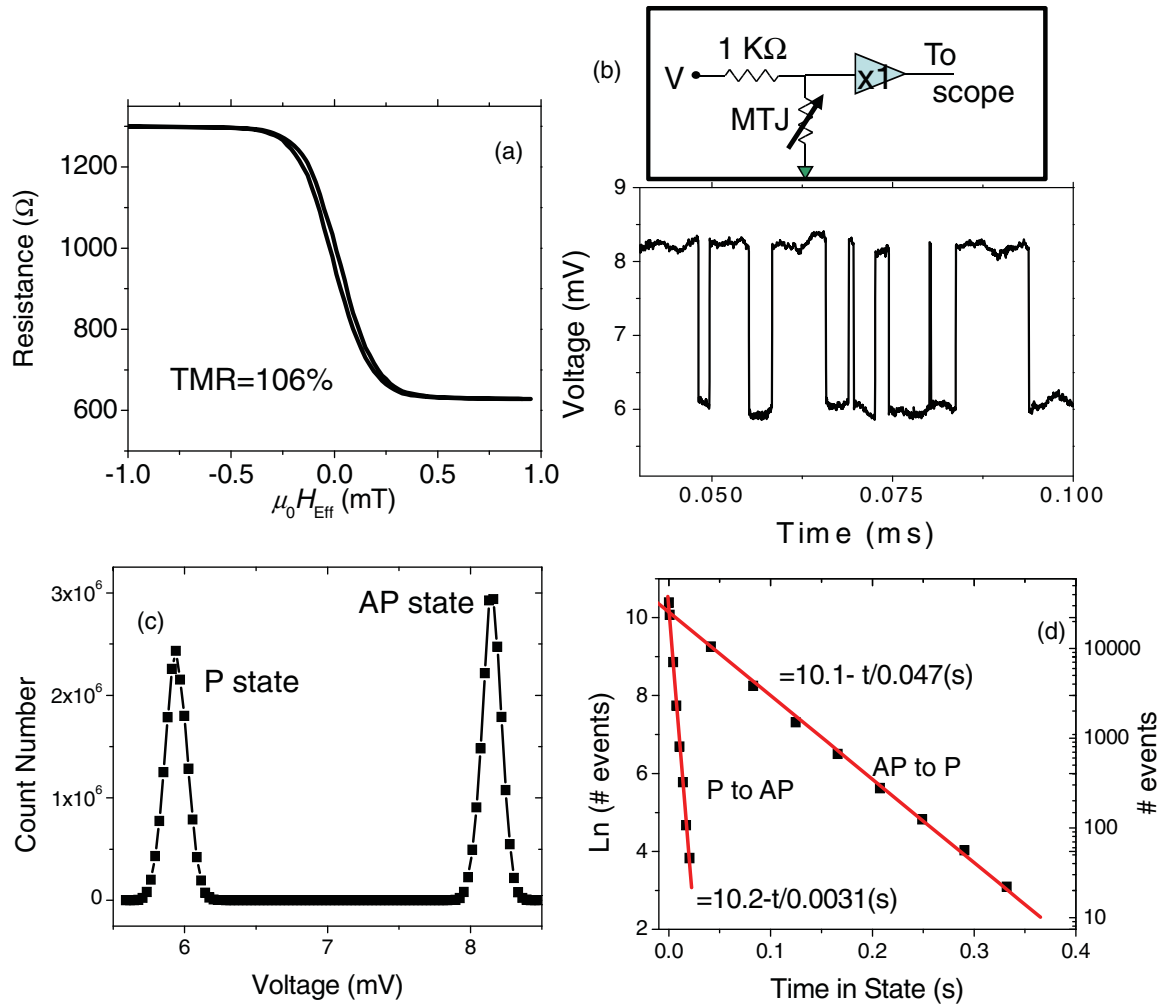
FIG. 1. (Color online) (a) Experimental TMR curve for the device shown here taken with a 5-μA current bias. The coupling field H_{coup} (=−0.9 mT at $T = 303$ K) between the CoFeB layers has been subtracted, as it is in all subsequent data. In all following data, we define H_{Eff} = (H_{applied} −H_{coup}). (b) A small section of an experimental time trace showing two-state switching for $\mu_0 H_{\text{Eff}} = 0$ mT. The voltage across the device corresponds to $V^{\text{AP}} = 8$ mV and $V^{\text{p}} = 6$ mV. The device is incorporated into a voltage divider circuit, so the difference in the voltages for the P and AP states does not correspond to the TMR value of the device. The full time trace consists of 32 Mpts and captures a roughly 4×10^4 transitions. (measurement schematic) The sampling rate of the scope is set so that a high number of transitions is obtained, while the sampling rate is a minimum of 200 times faster than the relaxation rate, so that short dwell time events are not missed. (c) A histogram of the full time trace of the measured voltage across the device shown in (b). The bimodal structure indicates that the device is well described by simple two-state switching with no evidence of an intermediate state being present. (d) Representative data showing the histogram of the time ($\mu_0 H_{\text{Eff}} = -0.2$ mT) the device remains in the P and AP states. The fits to the data give $\tau^{\pm}$ through Ln(N) $\sim -t/\tau^{\pm}$ where N is the number of events.

layer thermally stable. From the wafer-level average (resistance•area) = 5 Ω-μm^2 of the starting stack and the average device resistance of 950 Ω, we estimate that the actual device dimensions are 20% larger than their nominal values, which is expected through fidelity loss in the pattern transfer via ion milling. The devices have uniaxial anisotropy predominantly due to the magnetostatic shape anisotropy. For the 60 × 90 nm^2 devices used here, the easy axis is along the device long-axis with a typical anisotropy field of $\mu_0 H_{\text{k}}$ = 4 mT to 6 mT. As evidenced by the nonhysteretic TMR curve in Fig. 1(a), the device is thermally unstable and retains the full TMR value. In all measurements reported below, the applied field H_{App} is applied along the nominal easy axis of the device.

The experimental measurement setup is shown in Fig. 1(b). A constant voltage is applied to a circuit in which the MTJ acts as variable resistor in series with a 1 KΩ resistor, with the voltage V across the MTJ being monitored through a buffer amplifier by a storage oscilloscope (bandwidth = 2.5 GHz). The buffer serves to isolate the relatively low impedance (50 Ω) scope from the high impedance MTJ. The practical bandwidth of the circuit is limited to roughly 50 MHz due to the resistance-capacitance time-constant associated with the high impedance MTJ and the capacitance of the cabling. The state of the device, parallel (P) or antiparallel (AP), is monitored through the real-time voltage measured across the MTJ, an example of which is given in Fig 1(b). As is shown in Fig. 1(c), the voltage distribution is bimodal
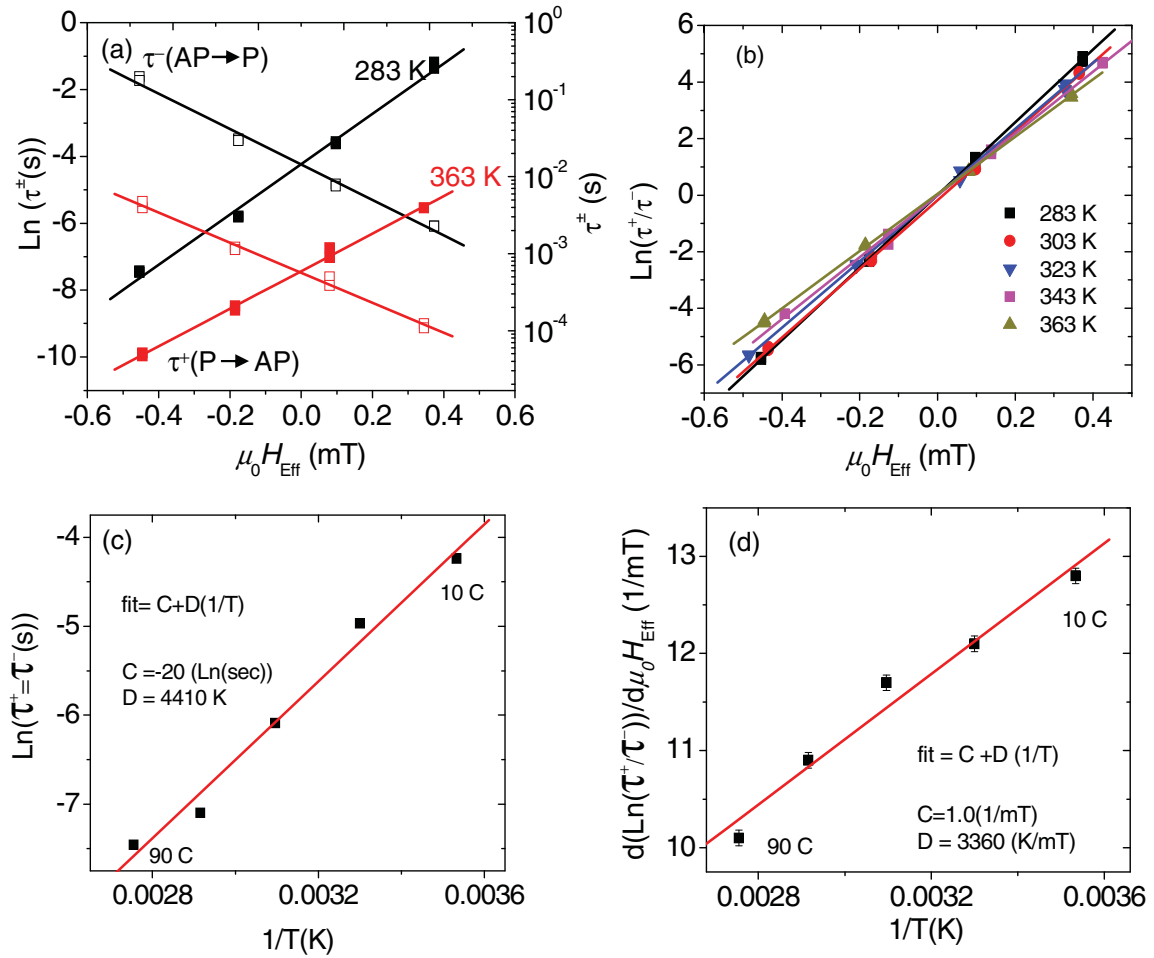
FIG. 2. (Color online) (a) Measured relaxation times for both τ^+ [the P-to-AP (■) transition] and τ^- [the AP-to-P (□) transition] as functions of field for $T = 283$ K and 363 K (other temperatures are not shown for clarity). (b) Ratio of the relaxation times as a function of field for T ranging from 283 K to 363 K along with linear fits. We define $\mu_0 H_{Eff} = 0$ mT as the field for which $\tau^+ = \tau^-$. The value of $\mu_0 H_{Coup}$ changes slightly with T ($\approx$0.002 mT/K), requiring different values of H_{Coup} to be subtracted from H_{App} for each temperature. (c) The values of τ^{Equal} vs $1/T$. The slope of this line gives E_0 and its intercept Ln(τ_0). (d) $d(Ln(\tau^+/\tau^-))/(d\mu_0 H_{Eff})$ vs $1/T$, the error bars are determined from the fits in (b).

with no intermediate states being present, and as such, the device is well described as a bistable system. The relaxation time $\tau^\pm$ of the free-layer magnetization at a particular applied field is determined by fitting exp(-$t/\tau^\pm$) to a histogram of the times the device spends in a particular state (where t is time and the superscript $+(-)$ denotes the P to AP (AP to P) relaxation time, respectively) as shown in Fig 1(d). Throughout this article, the histograms are created from a minimum of 10^3 transitions, with a typical value being more than 10^4. In Fig. 1, the voltage across the device is 6 mV (8 mV) in the P (AP) state, respectively. We consider this to be essentially equivalent to $V = 0$ V, the validity of which is verified below.

In the Néel-Brown (NB) model,[24] the measured relaxation time (dwell time) of a magnetic particle with uniaxial anisotropy at $V = 0$ V as a function of applied field is given by

$$\tau^\pm = \tau_0 \exp\left(\Delta\left(1 \pm \frac{H_{Eff}}{H_k}\right)^n\right), \quad (1)$$

where τ_0 is the effective attempt time, $\Delta = E_0/k_B T$, E_0 is the energy barrier, k_B is Boltzmann's constant, T is temperature,

and H_{Eff} is the total effective field applied along the easy axis of the device. In the following we take $n = 2$, which is appropriate for a single domain particle with uniaxial anisotropy.[25] We first analyze the relaxation times as a function of field and temperature (Fig. 2(a)) within the limit of $H_{Eff}/H_k \ll 1$ of Eq. (1):

$$Ln(\tau^\pm) = Ln(\tau_0) + \Delta\left(1 \pm \frac{2H_{Eff}}{H_k}\right). \quad (2)$$

A fundamental prediction of Eq. (2) is that, assuming Δ for the P and AP states are equivalent, the relaxation times should be symmetric with respect to H_{Eff}, (i.e., $|d\tau^\pm/dH_{Eff}|$ for the two states are equal). We use this as a criterion of device suitability, as it is not met by all structures. In many devices, symmetric behavior can be induced by rotating the device with respect to H, suggesting that the fabricated device is not parallel to the pin direction, although this was not necessary for the data presented here. In other cases, simple rotation does not strongly affect the asymmetric behavior, suggesting that it results from lithographic imperfections or intrinsic film

defects. For all data shown here, two separate time traces are recorded and analyzed under each bias condition in order to ensure repeatability of the measurements, with the resulting data points typically overlapping.

A. Temperature dependence

We can gain insight into the thermally activated nature of the switching by measuring the relaxation times as a function of temperature. Figure 2(a) shows the values of $\tau^{\pm}$ as a function of H_{Eff} for $T = 283$ K and 363 K. Increasing temperature serves to reduce the relaxation times of both states and also acts to change the coupling between the layers slightly. Figure 2(b) shows the ratio of the relaxation times $Ln(\tau^+/\tau^-)$ as a function of H_{Eff} for several different temperatures and shows that another effect of temperature is to change $d(Ln(\tau^+/\tau^-))/dH_{Eff}$.

Within the NB model discussed above, at $\mu_0 H_{Eff} = 0$ T the relaxation times for the two states are equal, with a value τ^{Equal} given by

$$Ln(\tau^{Equal}) = Ln(\tau_0) + \frac{E_0}{k_B T}. \qquad (3)$$

A plot of τ^{Equal} vs $1/T$ is shown along with a fit in Fig. 2(c), which gives $Ln(\tau_0(s)) = -20 \pm 1.0$ (Ln(s)) (corresponding to $\tau_0 = 0.8$ ns to 6 ns) and $E_0 = (0.38 \pm 0.027)$ eV (corresponding to $\Delta(T = 300$ K$) = 15 \pm 1.0$). This value of τ_0 should be taken as a lower limit on its actual value, as it is possible that E_0 itself is temperature dependent, and a simple linear decrease in the value of E_0 with T would serve to lower the apparent value of τ_0, which cannot be accounted for in this measurement. Interestingly, we find that this RT value of τ_0 is on the same order as that reported for a nanoparticle at T = 4K.[19,20]

Varying the temperature also allows us to determine H_k as well as estimate the effective switching volume of the device, which could be different from its physical volume if switching is being seeded by fluctuations in a subset of grains within it. In Fig. 2(d) we plot $d(Ln(\tau^+/\tau^-))/(d\mu_0 H_{Eff})$ as a function of $1/T$ along with a linear fit. From Eq (1), the slope of this function, i.e., $d^2(Ln(\tau^+/\tau^-)/d(1/T)d(\mu_0 H_{Eff})$, is $4E_0/(k_B \mu_0 H_k) = (3360 \pm 130)$ (K/mT), corresponding to $\mu_0 H_k = (5.2 \pm 0.18)$ mT using the value of E_0 determined above. This is in good agreement with the values from single domain modeling of $\mu_0 H_k \approx 4$ mT to 6 mT, depending of the exact aspect ratio assumed for the actual device. Using the relation $E_0 = \mu_0 H_k M_s \Omega/2$, where Ω is the volume inducing switching and the wafer-level value of $M_s \approx 1000$ kA/m, we find $\Omega = 2.3 \times 10^4$ nm^3, which is somewhat larger than the expected physical device volume of 1.3×10^4 nm^3, supporting the assertion that the device is switching as a single domain entity rather than via nucleation. In total, these data give strong evidence for the device acting as a single domain object being thermally activated over a single energy barrier, and that its switching is well described by the NB model. The methodology and recent improvements in TMR values now allows such measurements to be performed at RT and low-bias values, so STT effects can be neglected.
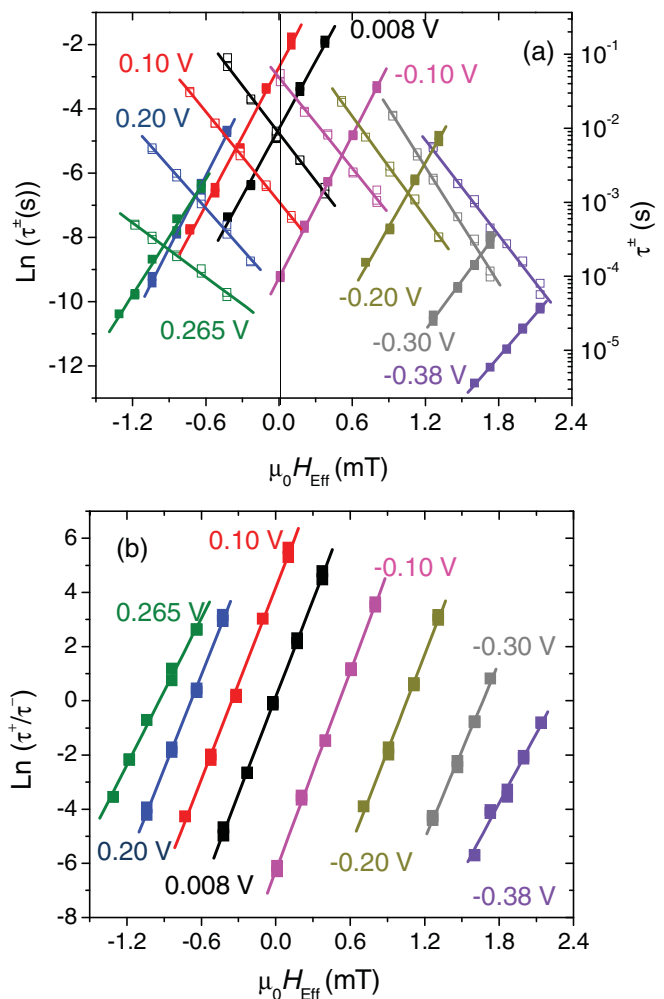

FIG. 3. (Color online) (a) Summary of the measured relaxation times at $T = 303$ K for both τ^+ (the P-to-AP (■) transition) and τ^- (the AP-to-P (□) transition) as a function of H_{Eff} for several different applied voltages, as indicated in the plot, along with linear fits. (b) $d(Ln(\tau^+/\tau^-))/(d\mu_0 H_{Eff})$ for the same applied voltages along with linear fits.

B. Voltage Dependence

We now turn our attention to the influence of voltage V on the relaxation times as a function of H_{Eff}, shown for a range of $V(-0.38$ V to 0.26 V) in Fig. 3(a) for $T = 303$ K. For voltages outside this range, the relaxation times were outside the bandwidth of the measurement circuit. Combined, these data represent the analysis of well over 10^6 individual switching events. The relaxation times must be compared and analyzed at a constant voltage, as the STT in MTJs is a voltage-driven process,[3,6] but for a given current bias, the voltages across the P and AP states are significantly different. To account for this, we first measure τ^- (the relaxation time for the AP to P transition) for a given current and then increase the current to induce the same voltage across the device while in the P state and then measure τ^+. Hence, the values of $\tau^{\pm}$ for a given V and H_{Eff} shown in Figs. 3 and 4 are taken from two different time traces.

The data in Fig. 3 show that the effects of V are significant, which can be most easily seen by comparing the values of
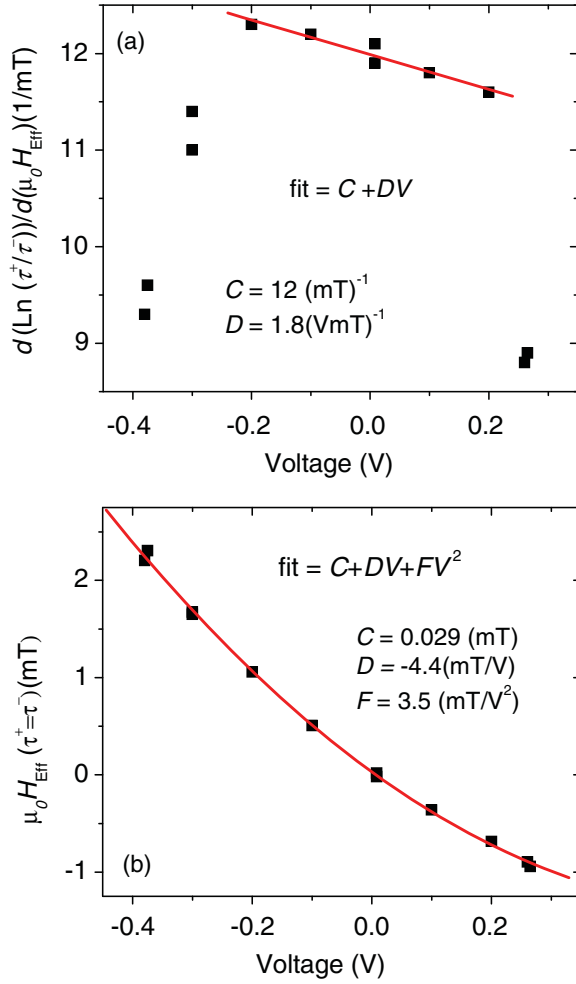
FIG. 4. (Color online) (a) Measured slopes of the data in Fig. 3(b), $d(\text{Ln}(\tau^+/\tau^-))/(d\mu_0 H_{\text{Eff}})$ vs applied voltage along with a linear fit for $|V| < 0.2$ V. (b) The measured value of H_{Eff}-intercept of the data in Fig. 3(b) along with a quadratic fit. The error bars in determining $\mu_0 H_{\text{Eff}}(\tau^+ = \tau^-)$ are ± 0.025 mT and are smaller than the data points.

$\tau^\pm$ at $\mu_0 H_{\text{Eff}} = 0$ mT. For $V = 8$ mV, the relaxation times for $\mu_0 H_{\text{Eff}} = 0$ mT are $\tau^\pm \approx 10$ ms. For $V = +0.1$ V, τ^- has been decreased by roughly a factor of 10, while τ^+ has been increased by roughly the same factor, indicating that the voltage roughly stabilizes the P state and destabilizes the AP state equivalently. For $V = -0.1$ V the situation is very different. While τ^- has now been increased by a factor of 10, τ^+ has been decreased by roughly a factor of 100. These variations are the combined effects of the in-plane and field-like spin-transfer torques, acting to alter the effective temperature and effective barrier between the two states, which are quantitatively analyzed below.

We analyze the relaxation times within a NB model modified to include the effects of the spin-transfer torques[18,26,27]

$$\tau^\pm = \tau_0 \exp\left(\Delta\left(1 \pm \frac{V}{|V_{c0}^\pm|}\right)\left(1 \pm \frac{AV + BV^2 + H_{\text{Eff}}}{H_k}\right)^2\right),$$

(4)

where $|V_{c0}^\pm|$ is the $T = 0$ K switching voltage. We allow for the field-like torque to have a linear and quadratic variation through the $(AV + BV^2)$ term, while the in-plane torque serves to increase the effective temperature through the $(1 \pm V/|V_{c0}^\pm|)$ term.[26,28,29] We use the convention that V is the voltage applied to the free layer while the fixed layer is held at ground.

In principle, we could directly fit the data in Fig. 3(a) with Eq. (4). However, we find that fitting the data in consecutive steps, as is done below, is more robust since it allows certain parameters to be removed from parts of the fitting process. The variation of $\text{Ln}(\tau^+/\tau^-)$ with V and H_{Eff} is given by

$$\left(\frac{1}{\Delta}\right)\text{Ln}\left(\frac{\tau^+}{\tau^-}\right) = \left[4 + 2V\left(\frac{1}{|V_{c0}^+|} - \frac{1}{|V_{c0}^-|}\right)\right]\frac{H_{\text{Eff}}}{H_k}$$
$$+ \left[\frac{4A}{H_k} + \left(\frac{1}{|V_{c0}^+|} + \frac{1}{|V_{c0}^-|}\right)\right]V$$
$$+ \left[\frac{4B}{H_k} + \frac{2A}{H_k}\left(\frac{1}{|V_{c0}^+|} - \frac{1}{|V_{c0}^-|}\right)\right]V^2$$
$$+ \left[\frac{2B}{H_k}\left(\frac{1}{|V_{c0}^+|} - \frac{1}{|V_{c0}^-|}\right)\right]V^3,$$

(5)

which is independent of τ_0, simplifying the analysis. To arrive at Eq. (5), we have done a Taylor expansion of the quadratic term in Eq. (4), which is appropriate since $\text{Ln}(\tau^\pm)$ depends linearly on H_{Eff} over the entire range of fields and voltages used here. Equation (5) predicts that $\text{Ln}(\tau^+/\tau^-)$ should vary linearly with H_{Eff}, with a slope that itself varies linearly with V and have an intercept along the ordinate that could be a fairly complicated function of voltage, depending on the relative strengths of the final three bracketed terms.

In obtaining Eq. (5) we have implicitly assumed that the value of Δ, and hence T, for a given voltage is identical for the P and AP states even though the power dissipated across the device is different. At the highest voltages, for which heating is expected to be more significant, this approximation improves since the TMR ratio decreases, and the resistances of the P and AP states converge (e.g., the device TMR is 38% at $V = 0.3$ V). Similarly, we have implicitly assumed that for a given voltage the effective τ_0 for the P and AP states are equivalent even though τ_0 is predicted to be a function of the magnetic damping parameter and T.[24] The modification of Δ through the in-plane torque is expected to be much more important in describing $\tau^\pm$ than a potential modification of τ_0 since Δ appears in the exponential term in Eq. (4). While there have been some attempts to account for Joule heating effects in MTJ structures,[17,30] we have found that including them in our analysis does not yield robust results but rather simply adds additional fitting parameters. In the following, the data are analyzed in such as way as to mitigate heating effects, and we show that the analysis is self-consistent over a significant voltage range and highlight where the inclusion of Joule heating in the model is possibly required.

The relaxation time ratios are shown in Fig. 3(b) along with linear fits, with their slopes given in Fig. 4(a) and intercepts along the field axis in Fig 4(b). As seen in Fig 3(b), the data are well approximated by a linear relationship between $\text{Ln}(\tau^+/\tau^-)$ and H_{Eff} over the entire range of V. The data in Fig. 4(a) show that the slope $d(\text{Ln}(\tau^+/\tau^-))/dH_{\text{Eff}}$ varies linearly with

voltage for $|V| < 200$ mV and decreases outside this range. Restricting the analysis to the linear portion of the data, within the modified NB model the data should have a $V = 0$ V intercept of $4\Delta/\mu_0 H_k = 12$ (1/mT) and a slope $\left(d^2(\mathrm{Ln}(\tau^+/\tau^-)/dH_{\mathrm{Eff}}\,dV)\right) = (2\Delta/\mu_0 H_k)\,(1/|V_{c0}^+| - 1/|V_{c0}^-|) = -1.8$ (mTV)$^{-1}$, its negative value being consistent with $|V_{c0}^+| > |V_{c0}^-|$ found in spin-torque switching experiments. Using these data we determine $(1/|V_{c0}^+| - 1|V_{c0}^-|) = -0.31$ (1/V), which is used below. The decrease in $d\left(\mathrm{Ln}(\tau^+/\tau^-)\right)/dH_{\mathrm{Eff}}$ at the higher voltages is consistent with device heating (which would directly lower Δ), a sublinear increase of the in-plane torque at large V as was measured in Ref. 16, or a combination of the two. More detailed measurements are needed to distinguish these potential contributions.

Figure 4(b) shows the measured values for the field intercept of $\mathrm{Ln}(\tau^+/\tau^-)$ as a function of voltage, along with a fit to a quadratic function. Using the measured value $(1/|V_{c0}^+| - 1/|V_{c0}^-|) = -0.31$ (1/V) and the approximation that $2 \gg |V|(1/|V_{c0}^+| - 1/|V_{c0}^-|)$, which is valid over the voltage range studied here, these data are described as

$$H(\tau^+ = \tau^-) = -\left\{\left[A + \frac{H_k}{4}\left(\frac{1}{|V_{c0}^+|} + \frac{1}{|V_{c0}^-|}\right)\right]V \right.$$
$$\left. + \left[B + \frac{A}{2}\left(\frac{1}{|V_{c0}^+|} - \frac{1}{|V_{c0}^-|}\right)\right]V^2\right\}. \quad (6)$$

It is important to note that Δ does not appear in this equation (within the approximation that Δ for the P and AP states is equal under equal V). Hence, in this analysis any voltage-dependent effects of Joule heating that act to lower Δ are minimized.

The data in Fig 4(b) have significant linear and quadratic components. From RT measurements of thermally stable devices having a similar area but elongated shape (50 × 150 nm^2) from the same wafer, we estimate that $|V_{c0}^+| \approx 0.9$ V and $|V_{c0}^-| \approx 0.7$ V under low-bias conditions.[31] Hence, the linear term evident in Fig. 4(b) largely arises from the modification of Δ from the in-plane torque, since $(\mu_0 H_k/4)\left((1/|V_{c0}^+| + 1/|V_{c0}^-|)\right) \approx 3.3$ mT/V. From this, we can estimate the value of $A \approx 1.1$ mT/V, which is substantially smaller than reported in Ref. 9 but similar to Ref. 11. The sign of A indicates that, in this sample, it acts to stabilize the P

(AP) state for $V > 0$ V (<0 V), respectively. Using this value for A and our determined value for $(1/|V_{c0}^+| - 1/|V_{c0}^-|)$, the quadratic term is dominated by the contribution of $B = (-3.2 \pm 0.16)$ mT/V^2, consistent with Refs. 14–16 but significantly less than in Refs. 8, 10, and 32. We note that while this analysis should be relatively insensitive to heating effects mentioned in regard to Fig. 4(a), a saturation in-plane torque would serve to increase the value of $|B|$. Using these determined values of A and B, we can conclude that the 6 mV to 8 mV bias used in deriving values for Δ, τ_0, and H_k above had no significant effect on their values.

The sign of B indicates that it favors AP alignment within the device independent of the sign of V, in agreement with Refs. 8 and 14–17. Over the voltages studied here, we see no indication of the field-like torque deviating from its quadratic dependence, unlike in Ref. 16. The fact that the quadratic term favors AP alignment in the device is a positive feature for STT-RAM devices in the low-voltage regime, since it is for P to AP switching that the required voltages are largest. However, in the large voltage regime, it can also be responsible for "back hopping."[17,33]

In summary, we have measured the relaxation times of a thermally unstable ferromagnetic nanoparticle as functions of temperature, field, and voltage. From low-bias measurements, the "intrinsic" properties of the device τ_0, Δ, and H_k can be determined. The effect of an applied voltage is to modify the relaxation times of the two states through both in-plane and field-like torques, which change the effective temperature and barrier height, respectively. By analyzing the results with a modified NB model, we are able to quantitatively determine the quadratic dependence of the field-like torque and estimate a linear contribution. The methods presented here should be easily applicable to other materials systems and devices, allowing systematic comparison between them.

*rippard@boulder.nist.gov

[1]J. Slonczewski, J. Magn. Magn. Mat. **159**, L1 (1996).

[2]J. Slonczewski and J. Sun, J. Magn. Magn. Mat. **310**, 169 (2007).

[3]J. Slonczewski, Phys. Rev. B **71**, 024411 (2005).

[4]L. Berger, Phys. Rev. B **54**, 9353 (1996).

[5]A. Kalitsov, M. Chshiev, I. Theodonis, N. Kioussis, and W. Butler, Phys. Rev. B **79**, 174416 (2009).

[6]C. Heiliger and M. D. Stiles, Phys. Rev. Lett. **100**, 186805 (2008).

[7]J. Xiao, G. E. W. Bauer, and A. Brataas, Phys. Rev. B **77**, 224419 (2008).

[8]A. M. Deac, A. Fukushima, H. Kubota, H. Maehara, Y. Suzuki, S. Yuasa, Y. Nagamine, K. Tsunekawa, D. D. Djayaprawira, and N. Watanabe, Nat. Phys. **4**, 803 (2008).

[9]O. Heinonen, S. Stokes, and J. Yi, Phys. Rev. Lett. **105**, 066602 (2010).

[10]M. H. Jung, S. Park, C.-Y. You, and S. Yuasa, Phys. Rev. B **81**, 134419 (2010).

[11]S. Petit, C. Baraduc, C. Thirion, U. Ebels, Y. Liu, M. Li, P. Wang, and B. Dieny, Phys. Rev. Lett. **98**, 077203 (2007).

[12]J. C. Sankey, P. M. Braganca, A. G. F. Garcia, I. N. Krivorotov, R. A. Buhrman, and D. C. Ralph, Phys. Rev. Lett. **96**, 227601 (2006).

[13]A. A. Tulapurkar, Y. Suzuki, A. Fukushima, H. Kubota, H. Maehara, K. Tsunekawa, D. D. Djayaprawira, N. Watanabe, and S. Yuasa, Nature **438**, 339 (2005).

[14]H. Kubota *et al.*, Nat. Phys. **4**, 37 (2007).

[15]C. Wang, Y.-T. Cui, J. Sun, J. A. Katine, R. A. Buhrman, and D. C. Ralph, Phys. Rev. B **79**, 224416 (2009).

[16]C. Wang, Y.-T. Cui, J. Sun, J. A. Katine, R. A. Buhrman, and D. C. Ralph, Nat. Phys. **7**, 496 (2011).

[17]S.-C. Oh *et al.*, Nat. Phys. **5**, 898 (2009).

[18]H.-J. Suh, C. Heo, C.-Y. You, W. Kim, T.-D. Lee, and K.-J. Lee, Phys. Rev. B **78**, 064430 (2008).

[19]W. Wernsdorfer, E. Orozco, K. Hasselbach, A. Benoit, B. Barbara, N. Demoncy, A. Loiseau, H. Pascard, and D. Mailly, Phys. Rev. Lett. **78**, 1791 (1997).

[20]I. N. Krivorotov, N. C. Emley, A. G. F. Garcia, J. C. Sankey, S. I. Kiselev, D. C. Ralph, and R. A. Buhrman, Phys. Rev. Lett. **93**, 166603 (2004).

[21]S. Krause, G. Herzog, T. Stapelfeldt, L. Berbil-Bautista, M. Bode, E. Vedmedenko, and R. Wiesendanger, Phys. Rev. Lett. **103**, 127202 (2009).

[22]C. P. Hancock, K. O'Grady, and M. El-Hilo, J. Phys. D **29**, 2343 (1996).

[23]D. Bedau, H. Liu, J. Z. Sun, J. A. Katine, E. E. Fullerton, S. Mangin, and A. D. Kent, Appl. Phys. Lett. **97**, 262502 (2010).

[24]W. F. Brown Jr., Phys. Rev. **130**, 1677 (1963).

[25]R. H. Victora, Phys. Rev. Lett. **63**, 457 (1989).

[26]Z. Li and S. Zhang, Phys. Rev. B **69**, 134416 (2004).

[27]Z. Li, S. Zhang, Z. Diao, Y. Ding, X. Tang, D. Apalkov, Z. Yang, K. Kawabata, and Y. Huai, Phys. Rev. Lett. **100**, 246602 (2008).

[28]R. H. Koch, J. A. Katine, and J. Z. Sun, Phys. Rev. Lett. **92**, 088302 (2004).

[29]J. Z. Sun, Phys. Rev. B **62**, 570 (2001).

[30]G. D. Fuchs, I. N. Krivorotov, P. M. Braganca, N. C. Emley, A. G. F. Garcia, D. C. Ralph, and R. A. Buhrman, Appl. Phys. Lett. **86**, 152509 (2005).

[31]R. Heindl, W. H. Rippard, S. E. Russek, M. R. Pufall, and A. B. Kos, J. Appl. Phys. **109**, 073910 (2011).

[32]S. Petit, N. de Mestier, C. Baraduc, C. Thirion, Y. Liu, M. Li, P. Wang, and B. Dieny, Phys. Rev. B **78**, 184420 (2008).

[33]J. Z. Sun, M. C. Gaidis, G. Hu, E. J. O'Sullivan, S. L. Brown, J. J. Nowak, P. L. Trouilloud, and D. C. Worledge, J. Appl. Phys. **105**, 07D109 (2009).